

# Quantum Efficient Detectors for Use in Absolute Calibration

Jessica Faust, Michael Eastwood, Betina Pavri, James Raney  
Jet Propulsion Laboratory  
California Institute of Technology  
Pasadena, CA 91109

## ABSTRACT

The trap or quantum efficient detector has a quantum efficiency of greater than 0.98 for the region from 450 to 900 nm. The region of flattest response is from 600 to 900 nm. The QED consists of three windowless Hamamatsu silicon detectors. The QED was mounted below AVIRIS to monitor the Spectralon panel for changes in radiance during radiometric calibration. The next step is to permanently mount the detector to AVIRIS and monitor the overall radiance of scenes along with calibration.

## BACKGROUND

The trap detector chosen has a quantum efficiency of greater than 0.98 for the region from 450 to 900 nm. The region of flattest response is from 600 to 900 nm. The model of trap detector chosen is the Graseby Optronics model QED-150. The QED consists of three windowless Hamamatsu silicon detectors. The increased quantum efficiency is due to two factors. First, each detector has a deeper depletion layer (than a typical photodiode) allowing for more efficient collection of photons in the red to NIR region. Second, the detectors are arranged at 45° angles to allow photons not absorbed by the first detector to reflect off at an angle that allows absorption by the second detector. Photons not absorbed at the second detector are absorbed by the third. The third detector is aligned such that any photons not absorbed are re-directed back toward the second and then first detectors. Thus, this design allows the system to act as if five detectors are in the optical path, raising the quantum efficiency of the device.

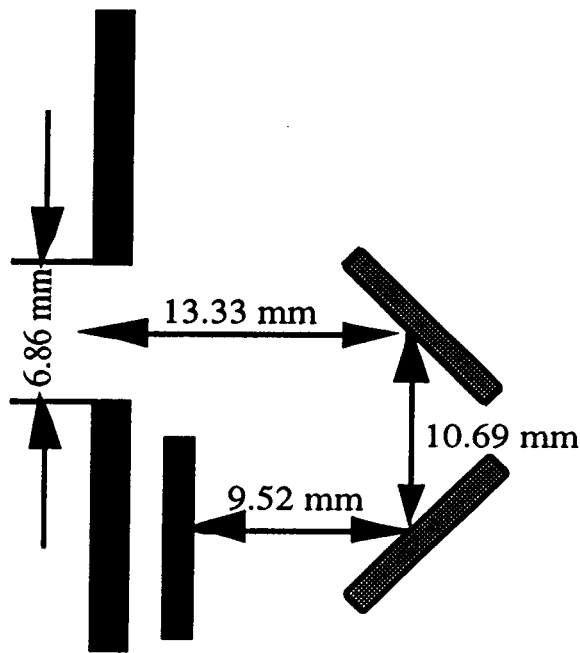


Figure 1. QED Detector Configuration

Two of the four AVIRIS spectrometers work within the range of the QED. Spectrometer A ranges from ~370 nm to 675 nm while spectrometer B's range is from ~665 nm to 1250 nm. A decision was made to limit the QED response to only one of the spectrometer ranges to better compare its data to the data from AVIRIS. The spectrometer data is integrated over the region for which the QED is filtered. Filters limiting the QED's response to the AVIRIS Spectrometer B wavelength range were chosen. A Melles-Griot bandpass (interference) filter with a  $780 \pm 2$  nm peak and  $20 \pm 4$  nm bandwidth limits the QED response. By the addition of RG695, a Schott cut-on filter, short wavelength leakage of 5% of the interference filter was reduced to 0.5%. Using a field spectrometer, the transmission of the each filter was measured to be 77.5% and 62% for the RG695 and Melles-Griot filters, respectively. In figure 2, a graph of the theoretical combination is given and shows a peak transmission of 58%.

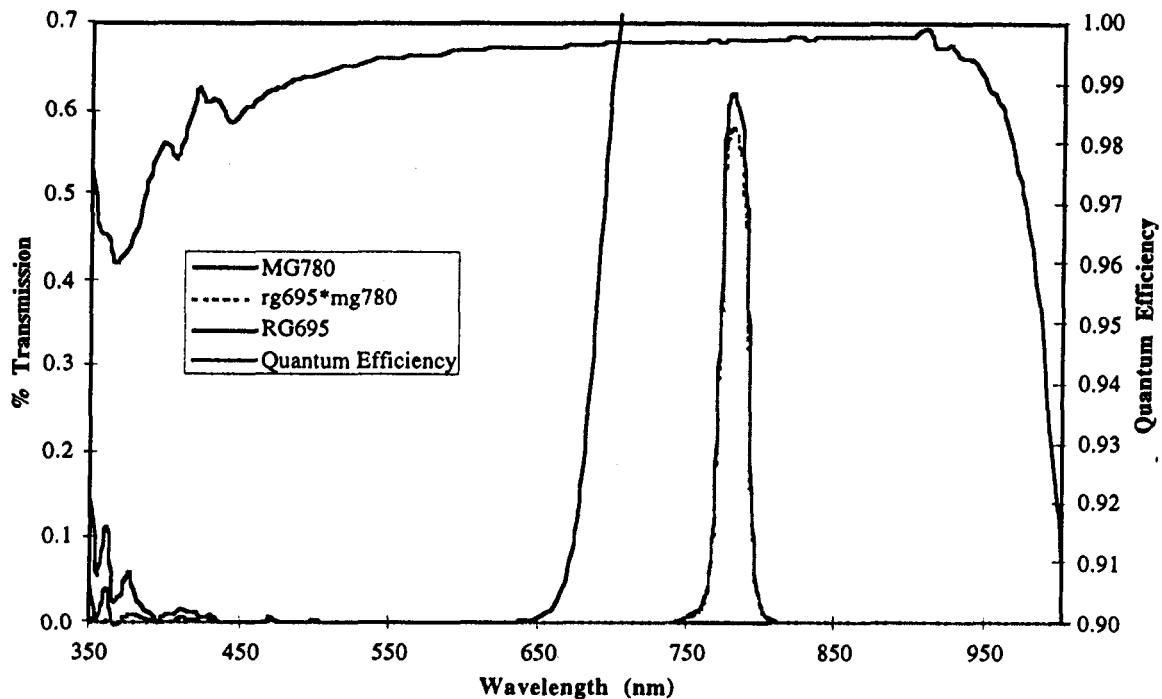


Figure 2. QED Response and Filter Transmission

A test was performed to determine the field-of-view of the QED without any apertures in place. The source --a 125 W bulb behind a diffuser and an aperture mask measuring approximate 5 mm in diameter-- was placed upon an optical table with the QED a known distance above it. Measurements were taken as the source was moved carefully two perpendicular axes within the QED's field-of-view. The result was the spatial response function of the detectors. Using this information, the field-of-view of the QED was determined to be approximately  $35^\circ$  in the horizontal axis. In the vertical axis the field-of-view was  $35^\circ$  in the upward direction and  $45^\circ$  in the downward direction. The reason for the change in the vertical axis is the angle of the first detector (see figure 1).

This field-of-view is too large for our application. The QED is to observe a Spectralon target (a 99% reflectance target from Labsphere). The target is 30.5 cm by 30.5 cm and will be viewed from approximately 1.5 m; therefore, the spot diameter seen by the QED would be 94 cm.

## SET-UP

The QED aperture has been limited to approximately  $5.5^\circ$  by the addition of a baffle assembly, which also serves as a filter retainer. The use of the first detector element was limited to the center 4 mm spot (of a  $1\text{ cm}^2$  detector). The baffle assembly was designed with three precision beveled apertures to reduce stray light effects. (See figure 3.) This baffle design allows for a 14.1 cm spot diameter on the target.

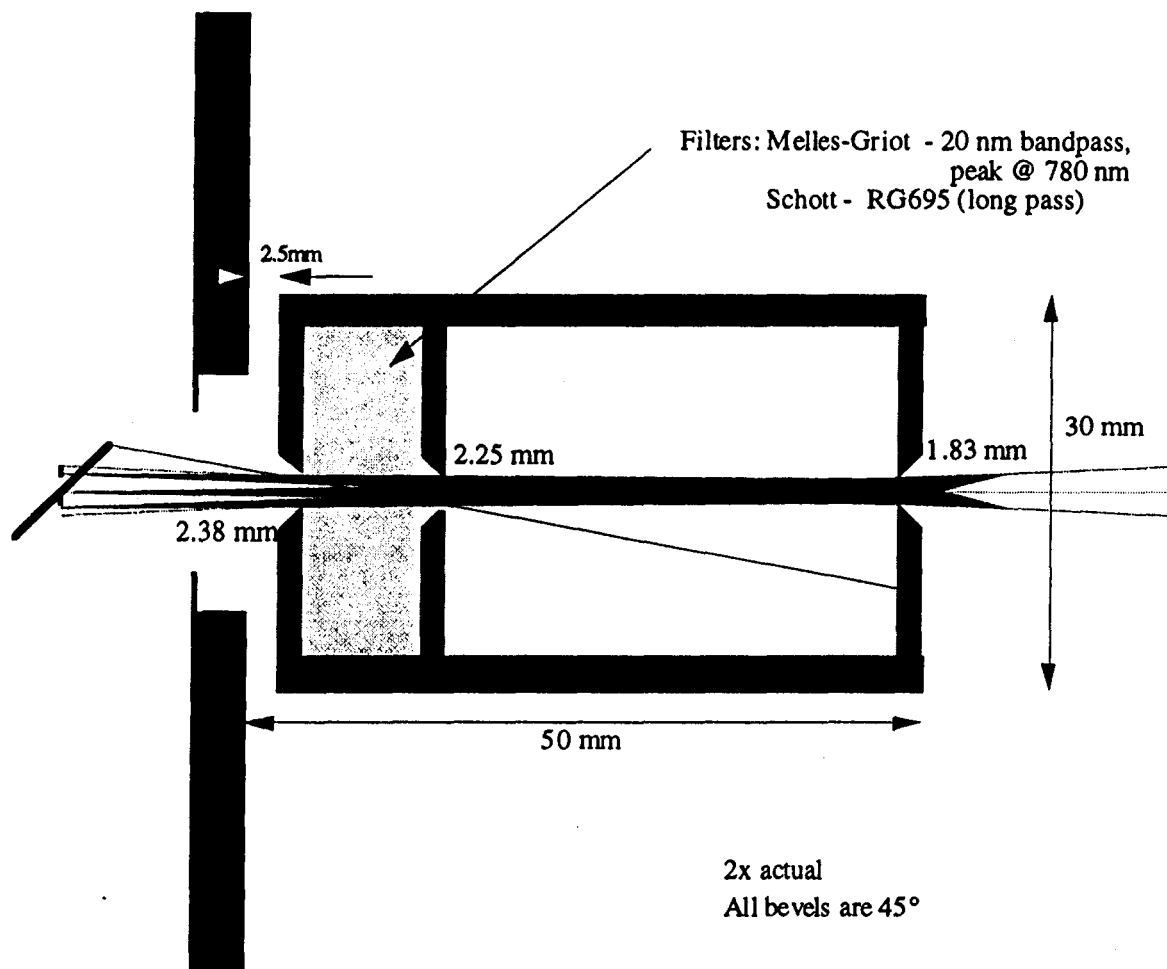


**Figure 3. Field-of-View Reduction Baffle Assembly**

During the 1997 flight season, the QED was removable and mounted on AVIRIS only during radiometric calibrations. This includes laboratory and field calibration. Figure 4 shows how the QED was put to use in monitoring the Spectralon target. The field target was carefully located beneath the AVIRIS, approximately  $5^{\circ}$  off the AVIRIS nadir looking view. For its initial use, the QED was aligned to the center of the target using a laser pointer and locked into position (mounted to the QED). For all subsequent tests, it was mounted in the same orientation for each calibration and whenever calibration is performed the target is aligned using the laser pointer attached to the QED. As a quick check, a *crosstrack* scan was run using the ground system to make sure that the target was aligned to the AVIRIS instantaneous field-of-view.

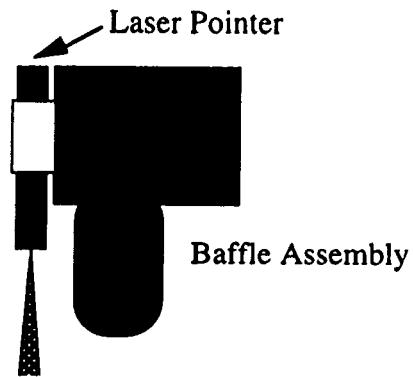


Figure 4. QED with laser pointer mounted

During the 1998 maintenance cycle, the QED will become a permanent part of the AVIRIS instrument. The QED will be hard mounted and incorporated into the AVIRIS data stream allowing for radiometric monitoring of calibration as well as flight scenes. The intent is that the QED will become an absolute radiometric calibration along with its current usage as a repeatable radiometric reference.

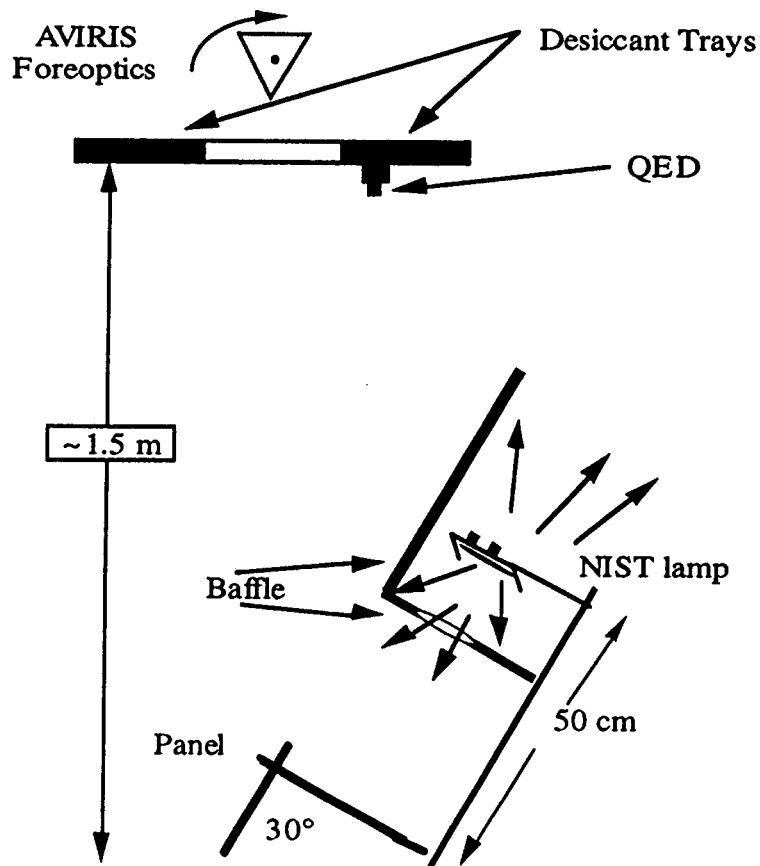


Figure 5. QED Current Configuration under AVIRIS

## ANALYSIS and RESULTS

Graseby Optronics (now, UDT Sensors) provides a performance specification for the QED as follows:

$$R = QE * (\lambda / 1239.5) \quad EQ. 1$$

$$I/P = QE * (\lambda / 1239.5) \quad EQ. 2$$

$$P = I / [ QE * (\lambda / 1239.5) ] \quad EQ. 3$$

where, *R* is Responsivity of the detector in A/W,  
*P* is the power input to the detector in Watts,  
*I* is the current output of the QED in Amperes,  
and  $\lambda$  is the wavelength of interest in nanometers.

Using the data taken with a point spectrometer, the transmission of the filter combination was approximated to a gaussian shape. The transmission peak was at 780.5 nm, with a full width half maximum of 18.9 nm, and a peak transmission of 63.6%. According to the data sent to us with the detector, the quantum efficiency at 780.5 nm is approximate 0.9973. In table 1 below, these values were used with the average readings taken by the QED of the spectralon panel when it was in place below AVIRIS.

DATE	Bulb	AVG Reading (A)	Flux (nW)
02/25/97	F-413	3.27E-09	5.2089
02/28/97	F-413	3.30E-09	5.2517
03/04/97	F-413	3.30E-09	5.2472
04/14/97	F-413	3.23E-09	5.1487
07/10/97	F-413	3.14E-09	4.9923
07/14/97	F-413	3.27E-09	5.2121
10/14/97	F-413	3.12E-09	4.9759
07/10/97	F-435	3.10E-09	4.9348
10/14/97	F-435	3.22E-09	5.1222
10/14/97	F-440	3.08E-09	4.9049

Table 1. QED Measurement Results

The theoretical values of flux are derived below by using the Irradiance ( $E_{bulb}$ ) and the reflectance ( $R_p$ ) of the Spectralon panel. Equation 4 describes the relationship between radiance and irradiance for a Lambertian scatterer such as the Spectralon panel is assumed to be. The area of the detectors is defined by simple geometry and the radius ( $r$ ) of the detector that has been illuminated is defined by the baffle described above. The area of the source is defined by the projection of the solid angle of the baffle where  $\theta$  is the half field-of-view of the baffle and  $r_p$  is the radius of the panel seen by the detectors.

$$L_s = E_{bulb}(\lambda) * R_p(\lambda) / \pi \quad EQ. 4$$

$$A_{det} = \pi * r^2 \quad EQ. 5$$

$$A_{src} = \pi * r_p^2 = \pi * z_{prime}^2 * \sin^2(\theta) \quad \text{EQ. 6}$$

$$\Phi = 1.05 \int_{740nm}^{810nm} \frac{L_s(\lambda) Area_{src} Area_{det} \cos \phi_1 \cos \phi_2}{z_{prime}^2} T_f(\lambda) d\lambda \quad \text{EQ. 7}$$

In equation 7, the angles,  $\phi_1$  and  $\phi_2$ , represent the angles of the Spectralon target and the detectors to the normal (to the floor). The factor of 1.05 is the correction factor for the Spectralon target. Betina Pavri has characterized several panels and found that the calibration values that are increased by a factor of 5% when the panel is viewed at a 30° angle. The variable  $T_f$  represents the filter transmission at each wavelength. The integrated flux expressed in equation 7 represents the theoretical values of flux that the detector should receive and record. Table 2 shows the values calculated using our field target and three different NIST FEL 1000 Watt lamps.

Lamp	Theoretical Flux (nW)
F-413	5.3662
F-435	5.7074
F-440	5.5930

Table 2. Theoretical Flux for Lamps Used in Field and Laboratory Calibrations

## RESULTS

The error between the theoretical QED response and the measured response is shown in figure 6. This chart reflects the error for all three FEL lamps.

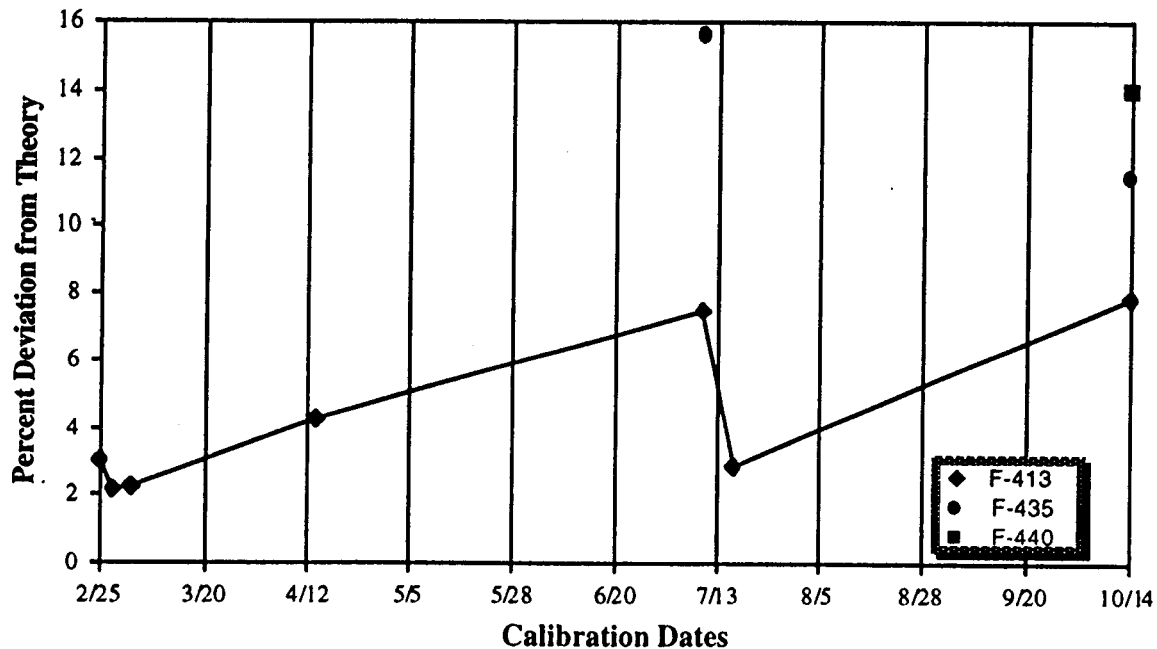


Figure 6. Error between theoretical and measured flux from QED for field calibrations

Several error contributions exist. The FEL lamps provided by Optronics are calibrated for use in the vertical position only. Using the lamps at a 30° angle to the vertical causes deterioration in the calibration numbers. The lamp's filament is not secured at both ends of the vacuum tube; therefore, when the lamp is used in a non-vertical position the filament sags. This causes the calibration of the lamps to be invalid after only a few hours of use was logged on each of them.

Another factor that contributes heavily to the errors seen with the F-413 bulb was the removal and replacement of the QED to its mounting each time it was used. The alignment procedure described above was used but it was difficult to position the target exactly the same way each time. Part of this is a factor of how AVIRIS is looking at the target. If the ER-2 has a light load (i.e., not much fuel on-board) then AVIRIS will be a little higher off the ground at slightly inclined toward the front of the aircraft. If the fuel load is heavy, then the ER-2 will be lower because of the additional weight. This factor also has to do with the errors seen.

One change in the AVIRIS instrument occurred in late July that accounts for the larger errors seen for the October 14 data. The new foreoptics door was installed while AVIRIS was on deployment at Ames Research Center. New desiccant trays for the foreoptics came with this door. The QED mount was on the trays and moved to the new trays but placed differently than before. Because of this error, the data taken with the QED was not as reliable as it had been beforehand.

Another source of error may be in several of the assumptions. When the spectralon panel is used at an angle, the calibration provided by Labsphere is off by a constant factor. This is mentioned in the Analysis and Results section. The Labsphere calibration is measured using a 8° hemispherical measurement at 45° to the normal of the target. A calibration of the reflectance is not possible unless the illumination were not normal to the panel, which is less than ideal. The 5% increase in reflectance values for a 30° use may need a slight adjustment because of this impossibility. This error contribution could be as much as 2-3 %.

Several activities are currently underway to ensure that these factors are reduced for the 1998 flight season. First, the use of the FEL lamps is being discontinued and NIST 200C lamps will be used once again. The 200C lamps are also 1000 Watts but are secured at both ends of the vacuum tube creating a tension in the filament that will keep it taut when in use. Second, the redesign of the field target is underway to ensure that AVIRIS and the QED will always be viewing it in the same geometry. Lastly, the QED will be hard-mounted and its data will be included in the data stream of AVIRIS.

The research described in this paper was carried out by the Jet Propulsion Laboratory under a contract with the National Aeronautics and Space Administration.